THERAPEUTIC ADVANCES in
Ophthalmology

Original Research

Choroid plexus asymmetry predicts decline in fundus blood flow in white matter hyperintensity patients: insights from SS-OCTA

Ther Adv Ophthalmol

2025, Vol. 17: 1–11

DOI: 10.1177/25158414251359581

Zeqi Shen, Weitao Yu, Jiawei Ye, Shouxuan Gao, Jie Zheng, Liang Yu, Faliang Gao, Chaoyang Hong* and Sheng Zhang*

Abstract

Background: This study aims to identify ocular fundus blood flow biomarkers, using swept-source optical coherence tomography angiography (SS-OCTA), that reflect choroid plexus (CP) changes in patients with white matter hyperintensities (WMHs).

Design: This is a retrospective analysis based on prospective data.

Methods: The study was an analysis of collected data from patients with WHMs who underwent multimodal magnetic resonance imaging (MRI) and SS-OCTA (FRESH-CSVD study, NCT06431711). Automatic segmentation was used to calculate the volumes of CP and WMHs. The bilateral CP asymmetry index was defined as the value of the difference in volume between the right and left CP, divided by the volume of the left CP. The association between SS-OCTA parameters, CP volume and its asymmetry index, and WMH volume (WMH-V) was analyzed using a LASSO-derived logistic regression model, with mediation analysis to explore their connections.

Results: The study included 240 eyes from 137 patients. A significant correlation was found between the bilateral CP asymmetry index and WMH-V ($\beta = -6.03$, 95% CI: −11.36 to −0.70, $p = 0.027$). WMH-V was correlated with the optic nerve head choriocapillaris perfusion area (ONH CC PA) ($\beta = -2.95$, 95% CI: −5.62 to −0.28, $p = 0.031$). The bilateral CP asymmetry index was also related to ONH CC PA ($\beta = 0.07$, 95% CI: 0.01 to 0.13, $p = 0.027$). Mediation analysis showed that WMH-V mediated 15.11% of the association between the bilateral CP asymmetry index and ONH CC PA ($p = 0.036$), but this mediation effect disappeared after adjusting for age.

Conclusion: These findings suggest that the morphological changes of the CP have a significant impact on the ONH blood flow in patients with WMHs. The ONH CC PA shows potential as a biomarker for detecting morphological changes of CP among WMHs patients.

Plain language summary

Our study used advanced imaging technology, SS-OCTA, to explore the relationship between the brain and the eyes. We discovered that in people with WMHs, the degree of CP asymmetry is linked to reduced blood flow in the choroidal capillaries and the extent of WMH damage.

Keywords: CP, SS-OCTA, WMHs

Received: 18 August 2024; revised manuscript accepted: 25 June 2025.

Correspondence to:
Sheng Zhang
Center for Rehabilitation Medicine, Department of Neurology, Zhejiang Provincial People's Hospital (Affiliated People's Hospital), Hangzhou Medical College, Shangtang Road No. 158, Hangzhou, Zhejiang 310014, China
zhangsheng@hmc.edu.cn

Chaoyang Hong
Center for Rehabilitation Medicine, Department of Ophthalmology, Zhejiang Provincial People's Hospital (Affiliated People's Hospital), Hangzhou Medical College, Shangtang Road No. 158, Hangzhou, Zhejiang 310014, China
hcy1999@sina.com

Zeqi Shen
Center for Rehabilitation Medicine, Department of Ophthalmology, Zhejiang Provincial People's Hospital (Affiliated People's Hospital), Hangzhou Medical College, Hangzhou, Zhejiang, China

Weitao Yu
The Second School of Clinical Medicine, Hangzhou Normal University, Hangzhou, Zhejiang, China

Jiawei Ye
School of Basic Medical Science and Forensic Medicine, Hangzhou Medical College, Hangzhou, Zhejiang, China

Shouxuan Gao
Center for Rehabilitation Medicine, Department of Neurology, Zhejiang Provincial People's Hospital (Affiliated People's Hospital), Hangzhou Medical College, Hangzhou, Zhejiang, China

Jie Zheng
Liang Yu
Department of Radiology, Zhejiang Provincial People's Hospital, Affiliated People's Hospital, Hangzhou Medical College, Hangzhou, Zhejiang, China

Faliang Gao
Center for Rehabilitation Medicine, Department of Neurosurgery, Zhejiang Provincial People's Hospital, Affiliated People's Hospital, Hangzhou Medical College, Hangzhou, Zhejiang, China

Current affiliation: Zeqi Shen is now affiliated with Postgraduate training base Alliance of Wenzhou Medical University (Affiliated People's Hospital), Hangzhou, Zhejiang, China

*These two authors contributed equally as co-corresponding authors.

Introduction

White matter hyperintensities (WMHs), affecting more than 95% of patients over 60 years of age,[1] have a causal relationship with headache, stroke, cognitive decline, dementia, and death.[2,3] Recent research found that morphological changes in the choroid plexus (CP) may lead to the development of WMHs.[4] Studies involving both animals and humans have found a connection between alterations in glymphatic function and the presence of WMHs, with the CP morphology reflecting changes in glymphatic system functionality.[5–7] This indicates that WMHs may arise from disruptions in the regulation of the glymphatic system by the CP.

Current clinical methods for measuring CP morphology and glymphatic function, such as structural magnetic resonance imaging (MRI) segmentation techniques, noninvasive diffusion tensor image analysis along the perivascular space (DTI-ALPS), and glymphatic MRI, are costly, technically demanding, and time-consuming.[8,9] Previous studies have found a close correlation between WMHs and ocular fundus blood flow.[10–12] The latest studies have identified a shared glymphatic pathway between the eye and the brain,[13–15] indicating that dysfunction in the glymphatic system can affect not only the brain but also the microvasculature of the ocular fundus.

Swept-source optical coherence tomography angiography (SS-OCTA) is the latest generation of rapid, noninvasive ophthalmic diagnostic tools for observing the microvasculature of the ocular fundus, including retina and choroid. Given its capabilities, SS-OCTA shows promise for early screening of WMHs patients. This study hypothesized that morphological changes in the CP of WMHs patients can be reflected through monitoring ocular fundus blood flow by SS-OCTA. In this study, we investigated the association among the CP, WMHs, and fundus microvascular structures to identify ocular fundus blood flow biomarkers indicative of CP changes in WMHs patients.

Methods

Ethical approval

This is a retrospective study of prospective data collection. Patients were enrolled in the from a clinical trial study from January 2023 to July 2024 to investigate the relationship among CP, WMH volume (WMH-V), and fundus blood flow. This clinical trial study is a single-center prospective observational study including adults aged ⩾18 who were diagnosed with cerebral small vessel disease (CSVD) and excluding those with MRI contraindications, serious head injury, or intracranial surgeries. Demographic characteristics, education levels, comorbidities, cognitive assessment scores (Mini-mental State Examination and Montreal Cognitive Assessment), brain imaging findings, and SS-OCTA imaging findings were evaluated. Exclusion criteria were who (i) had a history of intraocular surgery (except cataract surgery), ocular trauma, high refractive error (±6.00 D), high astigmatism (±3.00 D), glaucoma, and other retinal diseases; (ii) had neurological disorders with a clear impact on cognitive and neural functions, such as Down syndrome, Alzheimer's disease, Parkinson's disease, and acute stroke; (iii) had poor imaging quality of OCTA (signal strength < 6) or MRI that affected postprocessing or further analysis.

Optical coherence tomography angiography acquisition and analysis

The SS-OCTA machine (VG200I; Intalight, Inc., vangogh v3.0.188, Henan, China) includes a scanning source laser with a central wavelength of approximately 1050 nm and a scanning rate of 200,000 A-scan scans per second. This study investigates the blood flow parameters of the macula and optic nerve head (ONH) using a 6 × 6 mm area scanning mode to capture three-dimensional volume data. The grating scanning scheme has 512 consecutive horizontal B-scans. Each B-scan contains 512 A-scans. The vessel density of the radial capillary network (RPC), superficial vascular complexes (SVC) and deep vascular complexes (DVC), perfusion area (PA) of RPC, SVC, DVC and choriocapillaris (CC) in the macular and ONH, choroidal vascular index (CVI) and choroidal vascular volume (CVV) of the macular within the 6 × 6 mm scan mode of the Early Treatment of Diabetes Retinopathy Study (ETDRS) gird were measured. Each ring in the 6 × 6 mm scan mode has radii of 1, 3, and 6 mm. These measurements were obtained using the automatic measurement software equipped in the OCTA machine.

Brain magnetic resonance imaging acquisition and evaluation

All participants underwent MRI scans for diagnosing WMHs using an eight-channel phased array head coil on a 3.0 Tesla whole-body MRI

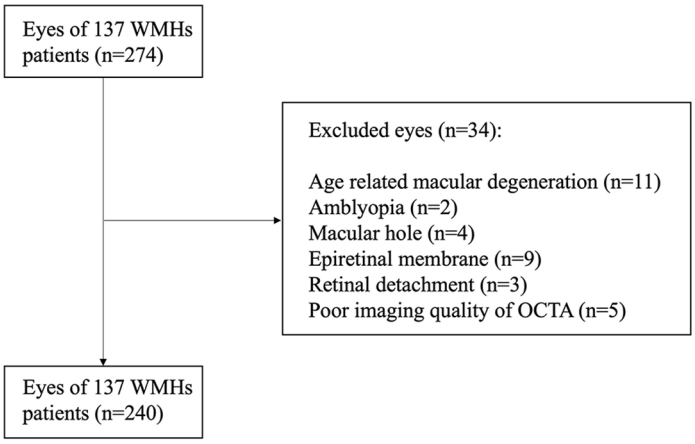

Figure 1. Flow chart of the inclusion and exclusion process.
OCTA, optical coherence tomography angiography; WMHs, white matter hyperintensities.

scanner (Discovery MR750 3.0T; GE Healthcare, Milwaukee, WI, USA). The detailed imaging protocol of brain MRI is shown in Supplemental Methods.

Evaluation of white matter hyperintensities volume

WMHs were defined as subcortical hyperintensities without cavitation on T2-weighted Fluid-Attenuated Inversion Recovery (T2-FLAIR) based on the recommendations of Standards for Reporting Vascular Changes on Neuroimaging (STRIVE-2).[16] According to the Fazekas scale, WMHs were divided into periventricular white matter hyperintensities (PWMHs) and deep white matter hyperintensities (DWMHs). To acquire WMH-V, all MRI scans were processed using the uAI Research Portal (United Imaging Healthcare, Shanghai, China).[17,18] The preprocessing included skull stripping, bias correction, and resampling images to $1 \times 1 \times 1\,mm^3$. T2-FLAIR images were segmented for white matter and further parcellated into 109 major regions of interests (ROI) according to the DK atlas.[19] The segmentation was done by a pretrained cascaded V-Nets, combining coarse localization and segmentation refinement.[20,21]

Evaluation of choroid plexus volume and choroid plexus asymmetry index

To acquire the CP volume, three-dimensional T1-weighted images (3D T1WI) were segmented for CP, following the same calculation methods as for WMHs. We specifically measured the following biomarkers related to CP: (i) bilateral CP volume (right CP, left CP, and total CP); (ii) bilateral CP asymmetry index: calculated as 1-(Right CP volume/Left CP volume); (iii) absolute value of bilateral CP asymmetry index.

Statistical analysis

For all quantitative data, we first performed normality tests. Data following a normal distribution were analyzed using *t*-tests, while data not meeting the normality assumption were analyzed using nonparametric tests. Quantitative variables were described as mean ± SD or interquartile range. We used linear regression and least absolute shrinkage and selection operator (LASSO) regression to screen for potential correlations between WMH-V, CP volume, bilateral CP asymmetry index, and SS-OCTA parameters in WMHs patients. Significant factors ($p < 0.05$) were included in multivariate logistic regression analysis. Mediation effect analysis was performed to assess the relationships among SS-OCTA parameters, CP volume, bilateral CP asymmetry index, and WMH-V. Statistical analyses were performed using SPSS version 26.0 (IBM, Chicago, Illinois, USA), R software version 4.2.2, and MSTATA software (www.mstata.com).

Results

Demographic and clinical characteristics

A total of 274 eyes from 137 WMHs patients were initially considered, with 37 eyes being excluded. Eventually, 240 eyes from 137 WMHs patients (71 females, 66 males) with an average age of 56.2 ± 11.5 years were included in the analysis (Figure 1). Among the WMHs patients, the

Table 1. Demographic characteristics in eyes of WMHs patients.

Characteristics	Eyes (*n* = 240)	Patients (*n* = 137)
Age, years, mean (SD)	56.23 (11.52)	57.66 (11.68)
Male, *n* (%)	117 (48.75)	66 (48.18)
History, *n* (%)		
Current smoking	74 (30.83)	42 (30.66)
Alcohol assumption	60 (25.00)	35 (25.55)
Hypertension	120 (50.00)	69 (50.36)
Diabetes mellitus	47 (19.58)	27 (19.71)
Hyperlipidemia	41 (17.08)	22 (16.06)
Ischemic stroke	54 (22.50)	33 (24.09)
Drug, *n* (%)		
Antihypertensive	124 (51.67)	72 (52.55)
Antidiabetic	45 (18.75)	27 (19.71)
Antiplatelet	73 (30.42)	44 (32.12)
Lipid-lowering	90 (37.50)	54 (39.42)
CSVD imaging marker		
WMH-V, ml, mean (SD)	7.58 (13.00)	8.37 (13.29)
PWMHs, *n* (%)	144 (60.00)	84 (61.31)
DWMHs, *n* (%)	193 (80.42)	112 (81.75)
Lacunes, *n* (%)	43 (17.92)	25 (18.25)
CMBs, *n* (%)	50 (20.83)	28 (20.44)
EPVS, *n* (%)	142 (59.17)	81 (59.12)
Brian atrophy, *n* (%)	135 (56.25)	80 (58.39)

CMB, cerebral microbleeds; CSVD, cerebral small vessel disease; DWMHs, deep white matter hyperintensities; EPVS, enlarged perivascular spaces; PWMHs, periventricular white matter hyperintensities; WMH-V, white matter hyperintensities volume.

WMH-V ranged from 0.01 to 88.31 ml. The proportions of WMHs patients with enlarged perivascular spaces (EPVS), lacunes, cerebral microbleeds (CMBs), and brain atrophy were 59.17%, 17.92%, 20.83%, and 56.25%, respectively. The demographic and clinical characteristics of the patients are shown in Table 1. No significant demographic differences were found in analyses conducted on both a per-eye and per-person basis.

Relationship between bilateral choroid plexus volume, choroid plexus asymmetry index, and white matter hyperintensities volume

The right CP volume (median value: 0.51 ml, IQR: 0.43–0.58 ml) was significantly larger than the left CP volume (median value: 0.48 ml, IQR: 0.40–0.56 ml) ($p = 0.012$). The median value of the bilateral CP asymmetry index was −0.04, with an index greater than 1 observed in 61.67% (148 out of 240) of cases.

Table 2. General linear regression and multivariate logistics regression analysis correlation coefficient between CP parameters and WMH-V in WMHs patients.

Characteristics	Univariate linear regression analysis			Multivariate logistic regression*		
	β Value	95% CI	*p* Value	β Value	95% CI	*p* Value
Total CP volume	0.13	0.01 to 0.25	0.041	−1.75	−8.43 to 4.93	0.607
Right CP volume	0.18	0.05 to 0.30	0.005	2.32	−6.30 to 10.95	0.597
Left CP volume	−0.01	−0.13 to 0.13	0.978	−11.44	−24.09 to 1.22	0.078
Bilateral CP asymmetry index	−0.21	−0.33 to −0.09	0.001	−6.03	−11.36 to −0.70	0.027

*Adjusted for age, gender, current smoking, alcohol assumption, hypertension, diabetes mellitus, hyperlipidemia, hyperlipidemia, ischemic stroke.
CP, choroid plexus; WMHs, white matter hyperintensities; WMH-V, white matter hyperintensities volume.

Table 3. Multivariate logistic regression correlation between WMH-V and 1–3 mm ONH CC PA in WMHs patients.

Characteristics	ONH CC PA		
	β Value	95% CI	*p* Value
WMH-V	−0.01	0.01 to 0.02	0.031
Age	−0.01	−0.21 to 0.01	0.002
Hypertension	−0.13	−0.28 to 0.03	0.106
Diabetes mellitus	−0.26	−0.45 to −0.06	0.001
Ischemic stroke	−0.03	−0.21 to 0.16	0.762

CC, choriocapillaris; ONH, optic nerve head; PA, perfusion area; WMHs, white matter hyperintensities; WMH-V, white matter hyperintensities volume.

Table 2 shows the association of bilateral CP volume and asymmetry index with WMH-V in WHMs patients. The results indicated that, except for the left CP volume, all CP-related parameters in WMHs patients were significantly correlated with WMH-V ($p < 0.05$). Multivariate logistic regression analysis, adjusted for covariates, revealed that the bilateral CP asymmetry index still exhibited a significant correlation with WMH-V ($\beta = -6.03$, 95% CI: −11.36 to −0.70, $p = 0.027$). For every 1% increase in the bilateral CP asymmetry index, the WMH-V decreased by 6.03 ml.

Relationship between white matter hyperintensities volume and optical coherence tomography angiography parameters

Demographic and clinical characteristics (age, male, current smoking, alcohol consumption, history of hypertension, diabetes mellitus, ischemic stroke, and medication history), along with 96 characteristics measured by OCTA, were included in the LASSO regression analysis to identify variables related to WMH-V (Supplemental Figure I). Variables selected through LASSO regression analysis were further included in multivariate Logistic regression analysis. This analysis revealed that WMH-V was significantly negatively correlated with the 1–3 mm ONH CC PA ($\beta = -0.01$, 95% CI: 0.01 to 0.02, $p = 0.031$) (Table 3). Except for 1–3 mm ONH CC PA, no other OCTA parameters, such as CVI and CVV, showed a significant association with WMH-V in our study.

Relationship between bilateral choroid plexus asymmetry index and optic nerve head choriocapillaris perfusion area

Demographic and clinical characteristics (age, male, current smoking, alcohol consumption, history of hypertension, diabetes mellitus, ischemic stroke, and medication history), along with 96

Table 4. Multivariate logistic regression of bilateral CP asymmetry index and 1–3 mm ONH CC PA in WMH patients.

Characteristics	ONH CC PA		
	β Value	95% CI	*p* Value
Bilateral CP asymmetry index	0.28	0.01 to 0.56	0.048
Age	−0.01	−0.01 to 0.01	0.043
Hypertension	−0.10	−0.27 to 0.06	0.214
Diabetes mellitus	−0.15	−0.36 to −0.05	0.144
Ischemic stroke	0.09	−0.10 to 0.29	0.354
Alcohol assumption	−0.11	−0.29 to 0.06	0.212

CC, choriocapillaris; CP, choroid plexus; ONH, optic nerve head; PA, perfusion area; WMHs, white matter hyperintensities.

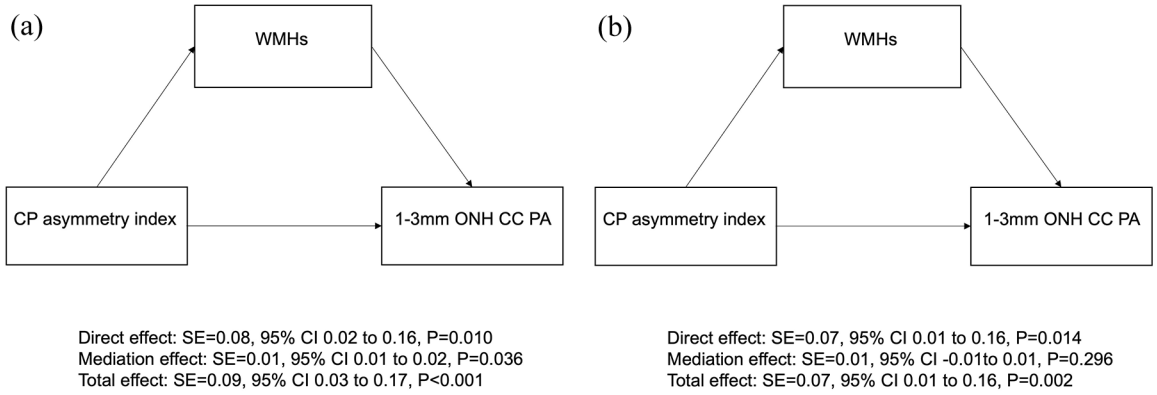

Figure 2. Mediation analysis before (a) and after adjusting for age (b).
CC, choriocapillaris; CP, choroid plexus; ONH, optic nerve head; PA, perfusion area; WMHs, white matter hyperintensities.

characteristics measured by OCTA, were included in the LASSO regression analysis to identify variables related to bilateral CP asymmetry index (Supplemental Figure II). Multivariate logistic regression analysis showed a significant association between the bilateral CP asymmetry index and 1–3 mm ONH CC PA (β = 0.28, 95% CI: 0.01 to 0.56, $p = 0.048$) (Table 4). For every 1% increase in the bilateral CP asymmetry index, the 1–3 mm ONH CC PA increased by 0.28 mm^2.

Mediation analysis

After conducting the LASSO regression analysis and the multivariate logistic regression analysis, no other CP indicators were found to be correlated with both WMH-V and ONH CC PA, except for the bilateral CP asymmetry index. The mediation analysis revealed that WMH-V mediates the relationship between the bilateral CP asymmetry index and ONH CC PA, with a mediation effect of 15.11% ($p = 0.036$) (Figure 2(a)). However, after adjusting for age, WMH-V no longer mediates this relationship ($p = 0.084$), and the bilateral CP asymmetry index directly affects ONH CC PA (direct effect: $p = 0.028$) (Figure 2(b)). Examples of two patients with different bilateral CP asymmetry indices, illustrating the bilateral CP asymmetry index, WMH-V, and ONH CC PA (Figure 3).

Discussion

In this study, we found that (i) the bilateral CP asymmetry index correlated with both WMH-V and the ONH CC PA; and (ii) there was a direct effect of the bilateral CP asymmetry index on the ONH CC PA. Notably, after adjusting for age,

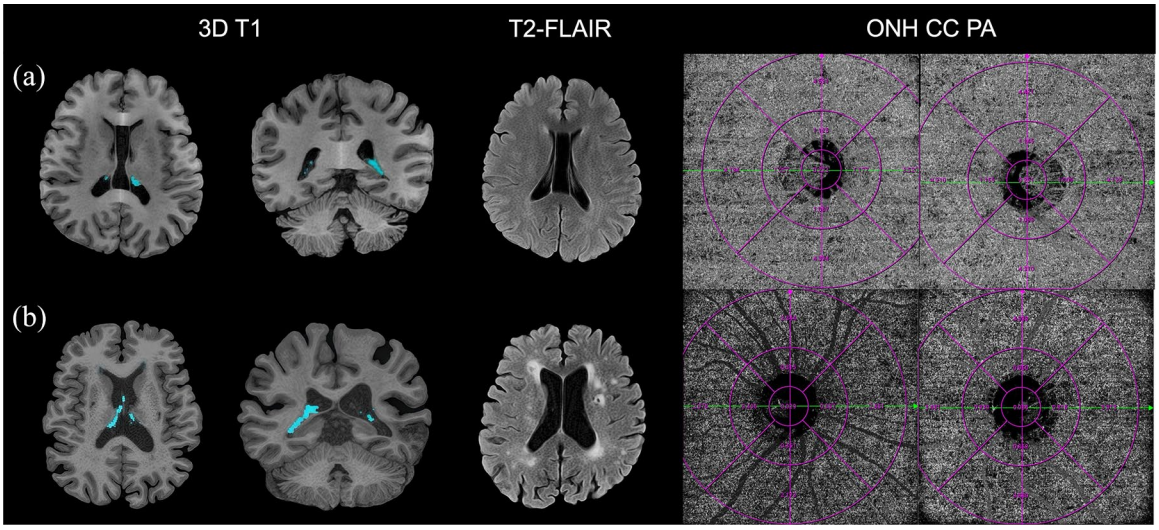

Figure 3. Examples of two patients with different bilateral CP asymmetry indices. Patient (a), a 49-year-old male, exhibited a bilateral CP asymmetry index of 0.079 as determined by 3D T1 MRI segmentation, which indicated a left-side predominance (blue area). His WMH-V was measured at 1.410 ml, with the ONH CC PA at 1–3 mm recorded at 1.112 mm^2 for the right eye and 1.102 mm^2 for the left eye. Patient (b), a 68-year-old male, presented a bilateral CP asymmetry index of –0.251 from the same 3D T1 MRI segmentation process, suggesting a right-sided dominance (blue area). His WMH-V was significantly higher, recorded at 17.380 ml. The ONH CC PA at 1–3 mm was noted at 0.439 mm^2 in the right eye and 0.766 mm^2 in the left eye.
CC, choriocapillaris; CP, choroid plexus; MRI, magnetic resonance imaging; ONH, optic nerve head; PA, perfusion area; SS-OCTA, swept-source optical coherence tomography angiography; WMH-V, white matter hyperintensities volume.

WMH did not mediate the relationship between these two factors.

In this study, we observed that in WMHs patients, the right CP volume was generally larger than the left, indicating a predominant right-sided CP dominance (61.67% vs 38.33%). This finding contrasts with previous studies in healthy individuals, where the left CP typically exhibits greater volume asymmetry over the right side.[22,23] This shift suggests pathological changes in CP morphology among WMHs patients. De Kovel et al. noted that genes associated with cell adhesion and immune responses are more expressed in the left CP, while cilia-related genes are more prominent in the right CP.[24] Ependymal cilia beating generates near-wall CSF flow, which is essential for glymphatic circulation and neuroblast migration.[25] Based on these findings, an increased right CP volume may indicate expansion of nonfunctional areas within the CP, potentially disrupting ciliary function and impairing CSF secretion and circulation.[26] Integrating these findings with previous studies on glymphatic dysfunction in WMHs development,[5–7] our findings suggest that bilateral CP asymmetry could indicate compromised ciliary function, impacting glymphatic function in WMHs patients.

Moreover, we discovered that changes in CP morphology not only contribute to WMHs but also lead to damage in retinal microvasculature, independent of WMHs. This damage may be attributed to dysfunction of the glymphatic system, which links the brain and the eye. Recent studies have found that the presence of the glymphatic system is not only in the brain but also within the eye, suggesting an interconnected glymphatic circulation system within the ocular structures. The ophthalmic glymphatic system may comprise retrograde and anterograde pathways. In the retrograde pathway, CSF produced by the CP enters the optic nerve sheath, collagenous fibers, and perivascular spaces around retinal vessels through the subarachnoid space, and finally enters the eye via the lamina cribrosa.[27–29] The anterograde pathway involves the retinal interstitial fluid (ISF) transporting retinal metabolic waste and neurotoxins, such as β-amyloid, along the axons of retinal ganglion cells. This transport is driven by the pressure difference across the lamina cribrosa and pupil constriction, and it utilizes AQP4 channels on the end feet of retinal Muller cells and astrocytes, exiting through the lamina cribrosa.[30,31] In summary, retinal ISF and CSF enter through the perivascular space around retinal arteries and transport waste out

through the perivenous space. They then enter the glymphatic circulation via dural lymphatic vessels.[32]

Thus, when the right nonfunctional area of the CP enlarges, cilia movement is impaired, CSF flow slows, and the cerebral glymphatic system is dysfunctional. This reduces the CSF entry rate into the eye via the optic nerve, the exchange rate of intraocular substances, and the transportation rate of retinal metabolic waste and neurotoxins by the ocular glymphatic system. Consequently, metabolic waste is more likely to deposit in retinal vessels, damaging the retinal microvasculature. Therefore, impaired glymphatic function could impact both the brain and retinal vasculature.[14] Our study speculates that CP morphological abnormalities, indicating compromised glymphatic system function, contribute not only to WMHs development but also disrupt the vascular system surrounding the optic nerve (Figure 4).

It is noteworthy that the mediation analysis in this study revealed that before adjusting for age, WMH-V acted as a mediator between the bilateral CP asymmetry index and the ONH CC PA. However, after accounting for age, the mediating effect of WMH-V disappeared. This is likely because aging influences morphological changes in the CP,[33] WMHs development,[34] and ocular fundus blood flow.[35] Age thus emerges as a significant factor influencing CP, WMHs, and fundus blood flow. Once age was considered, it was found that bilateral CP asymmetry index directly impacts ONH CC PA. This suggests that the decline in ocular fundus blood flow may not be solely attributed to WMHs. Rather, instead, alterations in CP morphology can affect both WMHs and ocular fundus blood flow concurrently.

Our study had several limitations. First, focusing on the eye as the unit of analysis might potentially overestimate the relationship between CP and ocular fundus blood flow. However, unlike previous studies that often included data from only one eye of WMHs patients, our study incorporated fundus blood flow data from both eyes, providing a more comprehensive understanding of changes in ocular fundus blood flow in WMHs patients. Second, given the cross-sectional nature and limited sample size of the study, future investigations should encompass larger sample sizes and longitudinal analyses of both eyes and individual patients. Longitudinal multicenter trials can monitor changes in CP morphology, WMH-V, and ONH CC PA over time. In addition, the impact of glymphatic metabolism-enhancing medications on CP morphology, WMH-V, and ONH CC PA in patients with WMHs warrants exploration to elucidate potential causal relationships. Third, this study excluded patients with fundus lesions. Given that retinal and choroidal abnormalities may influence ocular blood flow dynamics, our findings may not be generalizable to WMH patients with concomitant fundus pathology. Future studies should specifically address this subgroup to further elucidate potential interactions. Finally, our study was conducted at a single center using the VG 200I SS-OCTA, which offers a broader range of parameters for assessing fundus blood flow compared to other OCTA machines. This single-center design limited our ability to compare scanning results with different OCTA devices in other centers. Future studies should involve multicenter collaborations and validation with other OCTA devices.

For ophthalmologists, the detection of unexplained decreases in ONH CC PA or increases in non-perfusion areas using SS-OCTA could serve as a prompt to refer patients to a neurologist for WMH screening. For neurologists, identifying WMHs will assess the risk of choroidal capillary damage and monitor for ischemic optic neuropathy, while long-term observation of CC PA asymmetry indices helps prevent and monitor both ocular and cerebral lesions, enhancing patient care and risk stratification through this integrated approach.

In conclusion, the morphological changes in the CP significantly impact deep ONH blood flow in WMHs patients. Furthermore, our findings suggest that ONH CC PA has the potential to serve as a biomarker for CP morphological changes in WMHs patients.

Declarations

Ethics approval and consent to participate

All clinical investigations have been conducted according to the principles expressed in the Declaration of Helsinki. Written informed consent was obtained from all patients. The study protocol was approved by the Ethics Committee of Zhejiang Provincial People's Hospital (Approval number: KY2024050). Patients were enrolled in the FRESH-CSVD study (ClinicalTrials.gov: NCT06431711).

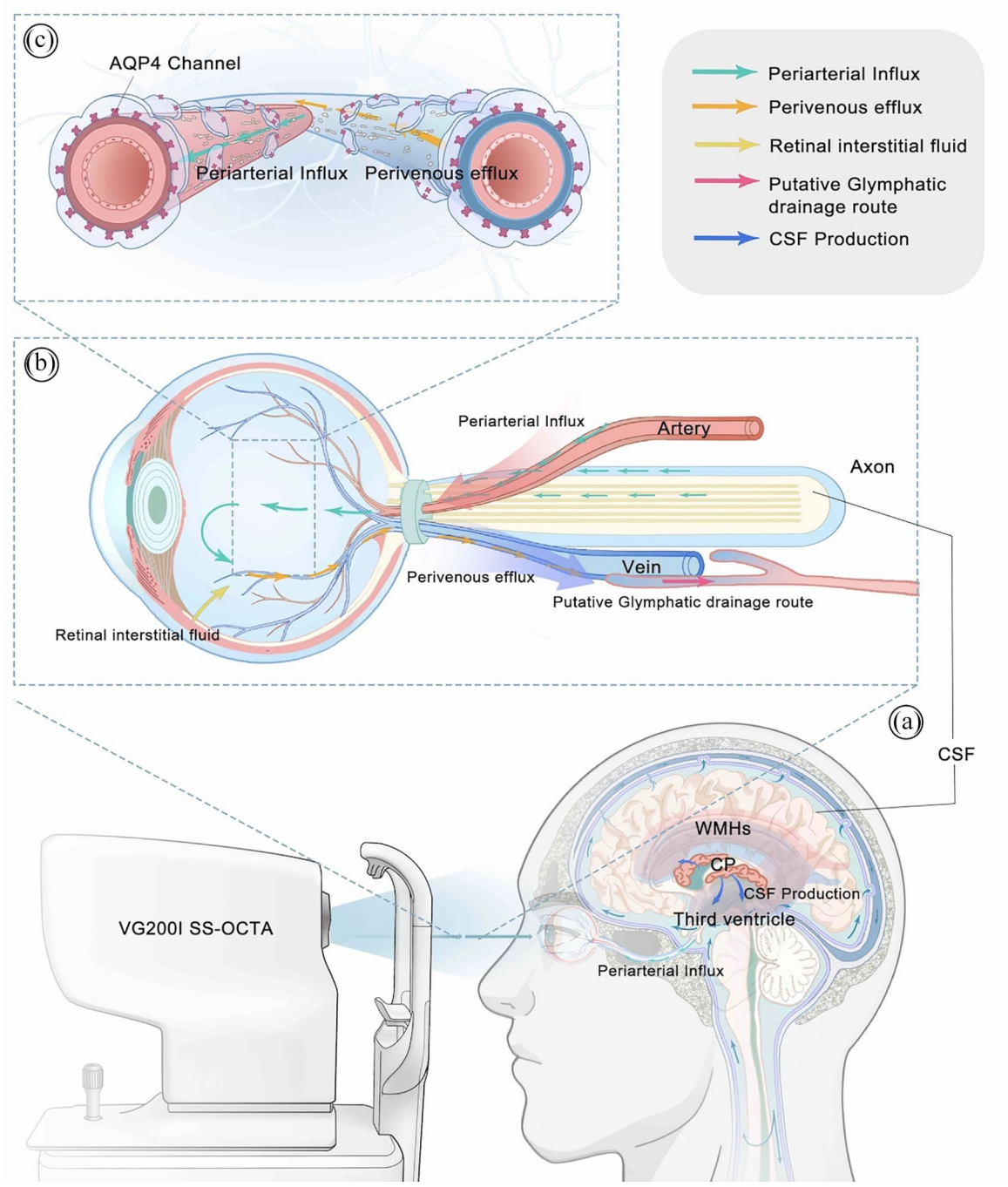

Figure 4. Mechanism of enlarged CP volume leading to decreased fundus blood flow in WMHs patients.
In patients with WMHs, enlargement of the nonfunctional area of the right CP leads to increased CP asymmetry, diminishing its capacity for CSF production and absorption (a). The disruption of CSF flow, a vital medium linking the brain-eye glymphatic system, not only results in glymphatic circulation impairments in the brain but also impacts ocular circulation (b). Dysfunction in ocular glymphatic processes contributes to a decreased rate of retinal metabolic waste transportation, ultimately leading to the accumulation of metabolic waste that damages the retinal microvasculature (c). The expansion of the nonfunctional area in the right CP hinders ciliary function, resulting in decreased CSF flow. This impedes the influx of CSF into the eye via the optic nerve sheath, perivascular space, and collagenous fibers (green arrow). Retinal interstitial fluid (yellow arrow) combines with CSF from the perivascular space of the retinal artery, facilitating the transfer of retinal metabolic waste and neurotoxins from the perivascular to the perivenous space of the retina. The diminished CSF flow also retards retinal metabolism, causing the accumulation of toxic substances (depicted as white deposits) and harm to the retinal microvasculature.
AQP4, Aquaporin 4; CP, choroid plexus; CSF, cerebrospinal fluid; WMHs, white matter hyperintensities.

Consent for publication
Not applicable.

Author contributions
Zeqi Shen: Writing – original draft.

Weitao Yu: Software; Supervision.

Jiawei Ye: Resources.

Shouxuan Gao: Resources.

Jie Zheng: Resources; Software.

Liang Yu: Resources; Software.

Faliang Gao: Resources.

Chaoyang Hong: Supervision.

Sheng Zhang: Conceptualization; Writing – review & editing.

Acknowledgements
None.

Funding
The authors disclosed receipt of the following financial support for the research, authorship, and/or publication of this article: This review was funded by Key research and development project of Zhejiang Provincial Department of Science and Technology (Grant No. 2021C03103), Zhejiang Provincial Natural Science Foundation of China (Grant No. LGF22H090020), and the Medical Health Science and Technology Project of the Zhejiang Provincial Health Commission (Grant No. 2022KY600 and 2024KY019).

Competing interests
The authors declare that there is no conflict of interest.

Availability of data and materials
The materials generated during the present review are available from the corresponding author on reasonable request. Considerations will be made based on the reasons for requesting the materials and the procedures for ensuring data privacy.

ORCID iDs
Zeqi Shen https://orcid.org/0009-0005-2697-8685

Weitao Yu https://orcid.org/0009-0009-4242-1923

Faliang Gao https://orcid.org/0000-0002-8170-2156

Sheng Zhang https://orcid.org/0009-0000-7035-9893

Supplemental material
Supplemental material for this article is available online.

References

1. Longstreth WT, Manolio TA, Arnold A, et al. Clinical correlates of white matter findings on cranial magnetic resonance imaging of 3301 elderly people: the cardiovascular health study. *Stroke* 1996; 27(8): 1274–1282.
2. Prins ND and Scheltens P. White matter hyperintensities, cognitive impairment and dementia: an update. *Nat Rev Neurol* 2015; 11(3): 157–165.
3. Icoz M and Akdeniz M. Peripapillary and subfoveal choroidal vascular index in patients with tension-type headache and migraine. *Indian Journal of Ophthalmology [Internet]*, https://journals.lww.com/10.4103/IJO.IJO_3370_23 (2024, accessed 9 March 2025).
4. Li Y, Zhou Y, Zhong W, et al. Choroid plexus enlargement exacerbates white matter hyperintensity growth through glymphatic impairment. *Ann Neurol* 2023; 94(1): 182–195.
5. Sabayan B and Westendorp RGJ. Neurovascular-glymphatic dysfunction and white matter lesions. *Geroscience* 2021; 43(4): 1635–1642.
6. Zhang W, Zhou Y, Wang J, et al. Glymphatic clearance function in patients with cerebral small vessel disease. *NeuroImage* 2021; 238: 118257.
7. Zhou Y, Xue R, Li Y, et al. Impaired meningeal lymphatics and glymphatic pathway in patients with white matter hyperintensity. *Adv Sci* 2024; 2402059.
8. Deike-Hofmann K, Reuter J, Haase R, et al. Glymphatic pathway of gadolinium-based contrast agents through the brain: overlooked and misinterpreted. *Invest Radiol* 2019; 54(4): 229–237.
9. Zhou Y, Cai J, Zhang W, et al. Impairment of the glymphatic pathway and putative meningeal lymphatic vessels in the aging human. *Ann Neurol* 2020; 87(3): 357–369.
10. Fu W, Zhou X, Wang M, et al. Fundus changes evaluated by OCTA in patients with cerebral small vessel disease and their correlations: a cross-sectional study. *Front Neurol* 2022; 13: 843198.

11. Zhou X, Li T, Qu W, et al. Abnormalities of retinal structure and microvasculature are associated with cerebral white matter hyperintensities. *Euro J Neurol* 2022; 29(8): 2289–2298.
12. Alten F, Motte J, Ewering C, et al. Multimodal retinal vessel analysis in CADASIL patients. *PLoS One* 2014; 9(11): e112311.
13. Tong XJ, Akdemir G, Wadhwa M, et al. Large molecules from the cerebrospinal fluid enter the optic nerve but not the retina of mice. *Fluids Barriers CNS* 2024; 21(1): 1.
14. Wang X, Lou N, Eberhardt A, et al. An ocular glymphatic clearance system removes β-amyloid from the rodent eye. *Sci Transl Med* 2020; 12(536): eaaw3210.
15. Mestre H, Kostrikov S, Mehta RI, et al. Perivascular spaces, glymphatic dysfunction, and small vessel disease. *Clin Sci (Lond)* 2017; 131(17): 2257–2274.
16. Duering M, Biessels GJ, Brodtmann A, et al. Neuroimaging standards for research into small vessel disease-advances since 2013. *Lancet Neurol* 2023; 22(7): 602–618.
17. Zhou L, Yang W, Liu Y, et al. Correlations between cognitive reserve, gray matter, and cerebrospinal fluid volume in healthy elders and mild cognitive impairment patients. *Front Neurol* 2024; 15: 1355546.
18. Wei J, Shi F, Cui Z, et al. Consistent segmentation of longitudinal Brain MR images with spatio-temporal constrained networks. In: *International conference on medical image computing and computer-assisted intervention* [Internet], http://link.springer.com/chapter/10.1007/978-3-030-87193-2_9 (2021, accessed 21 June 2024).
19. Arno K and Jason T. 101 Labeled brain images and a consistent human cortical labeling protocol. *Front Neurosci* 2012; 6(171): 171.
20. Hua R, Huo Q, Gao Y, et al. Segmenting brain tumor using cascaded V-nets in multimodal MR images. *Front Comput Neurosci* 2020; 14: 9.
21. Mu G, Lin Z, Han M, et al. Segmentation of kidney tumor by multi-resolution VB-nets. In: *2019 Kidney Tumor Segmentation Challenge: KiTS19* [Internet], http://www.researchgate.net/publication/336247962_Segmentation_of_kidney_tumor_by_multi-resolution_VB-nets (2019, accessed 21 June 2024).
22. Hering-Hanit R, Achiron R, Lipitz S, et al. Asymmetry of fetal cerebral hemispheres: in utero ultrasound study. *Arch Dis Child Fetal Neonatal Ed* 2001; 85(3): F194–F196.
23. Gilmore JH, Lin W, Prastawa MW, et al. Regional gray matter growth, sexual dimorphism, and cerebral asymmetry in the neonatal brain. *J Neurosci* 2007; 27(6): 1255–1260.
24. De Kovel CGF, Lisgo SN, Fisher SE, et al. Subtle left-right asymmetry of gene expression profiles in embryonic and foetal human brains. *Sci Rep* 2018; 8(1): 12606.
25. Siyahhan B, Knobloch V, de Zélicourt D, et al. Flow induced by ependymal cilia dominates near-wall cerebrospinal fluid dynamics in the lateral ventricles. *J R Soc Interface* 2014; 11(94): 20131189.
26. Choi JD, Moon Y, Kim HJ, et al. Choroid plexus volume and permeability at brain MRI within the Alzheimer disease clinical spectrum. *Radiology* 2022; 304(3): 635–645.
27. Wostyn P, Killer HE and De Deyn PP. Glymphatic stasis at the site of the lamina cribrosa as a potential mechanism underlying open-angle glaucoma. *Clin Exp Ophthalmol* 2017; 45(5): 539–547.
28. Jacobsen HH, Ringstad G, Jørstad ØK, et al. The human visual pathway communicates directly with the subarachnoid space. *Invest Ophthalmol Vis Sci* 2019; 60(7): 2773–2780.
29. Mathieu E, Gupta N, Ahari A, et al. Evidence for cerebrospinal fluid entry into the optic nerve via a glymphatic pathway. *Invest Ophthalmol Vis Sci* 2017; 58(11): 4784–4791.
30. Uddin N and Rutar M. Ocular lymphatic and glymphatic systems: implications for retinal health and disease. *Int J Mol Sci* 2022; 23(17): 10139.
31. Cao Q, Yang S, Wang X, et al. Transport of β-amyloid from brain to eye causes retinal degeneration in Alzheimer's disease. *J Exp Med* 2024; 221(11): e20240386.
32. Mogensen FLH, Delle C and Nedergaard M. The glymphatic system (En)during inflammation. *Int J Mol Sci* 2021; 22(14): 7491.
33. Damkier HH, Brown PD and Praetorius J. Cerebrospinal fluid secretion by the choroid plexus. *Physiol Rev* 2013; 93(4): 1847–1892.
34. Zhuang FJ, Chen Y, He WB, et al. Prevalence of white matter hyperintensities increases with age. *Neural Regen Res* 2018; 13(12): 2141–2146.
35. Wiącek MP, Modrzejewska M and Zaborski D. Age-related changes in retrobulbar circulation: a literature review. *Int Ophthalmol* 2020; 40(2): 493–501.